analytical chemistry

University of Texas Libraries

Subscriber access provided by University of Texas Libraries

Application of photothermal spectroscopy to in-situ studies of films on metals and electrodes

George H. Brilmyer, and Allen J. Bard

Anal. Chem., **1980**, 52 (4), 685-691• DOI: 10.1021/ac50054a023 • Publication Date (Web): 01 May 2002

Downloaded from http://pubs.acs.org on February 13, 2009

More About This Article

The permalink http://dx.doi.org/10.1021/ac50054a023 provides access to:

- Links to articles and content related to this article
- Copyright permission to reproduce figures and/or text from this article

ACS Publications
High quality. High impact.

Analytical Chemistry is published by the American Chemical Society. 1155 Sixteenth Street N.W., Washington, DC 20036

of greater increases in its sensitivity, because the limit in detection of temperature changes has been reported to be about 10^{-6} K (23). The PTS technique requires only simple instrumentation and is advantageous in terms of sample preparation, because it is unaffected by scattering losses. In addition, PTS would be useful for studying rough and porous surfaces which are difficult to examine by conventional spectroscopic techniques.

LITERATURE CITED

(1) G. H. Brilmyer, A. Fujishima, K. S. V. Santhanam, and A. J. Bard, *Anal. Chem.*, **49**, 2057 (1977).
(2) W. Benken and T. Kuwana, *Anal. Chem.*, **42**, 1114 (1970).
(3) W. R. Heineman and T. Kuwana, *Anal. Chem.*, **43**, 1075 (1971).
(4) W. N. Hansen and J. A. Horton, *Anal. Chem.*, **36**, 783 (1964).
(5) W. N. Hansen, T. Kuwana, and R. A. Osteryoung, *Anal. Chem.*, **38**, 1810 (1966).
(6) D. F. A. Koch, *Nature (London)*, **202**, 387 (1964).
(7) J. D. E. McIntyre, *Adv. Electrochem. Electrochem. Eng.*, **9**, 61-166 (1973).
(8) J. Kruger, *J. Electrochem. Soc.*, **110**, 654 (1963).
(9) W. Paik, M. A. Genshaw, and J. O'M. Bockris, *J. Phys. Chem.*, **74**, 4266 (1970).
(10) A. Rosencwaig, *Anal. Chem.*, **47**, 592A (1975).
(11) M. J. Adams, A. A. King, and G. F. Kirkbright, *Analyst (London)*, **101**, 73 (1976).
(12) V. R. B. Somoano, *Angew. Chem.*, **90**, 250 (1978).
(13) R. Tamamushi, *J. Electroanal. Chem.*, **65**, 263 (1975).
(14) W. E. Reid and J. Kruger, *Nature (London)*, **203**, 402 (1964).
(15) R. S. Sirohi and M. A. Genshaw, *J. Electrochem. Soc.*, **116**, 910 (1969).
(16) T. Takamura, K. Takamura, W. Nippe, and E. Yeager, *J. Electrochem. Soc.*, **117**, 626 (1970).
(17) D. M. Kolb and J. D. E. McIntyre, *Surf. Sci.*, **28**, 321 (1971).
(18) B. D. Cahan, J. Horkans, and E. Yeager, *Symp. Faraday Soc.*, **4**, 36 (1972).
(19) M. Stedman, *Chem. Phys. Lett.*, **2**, 457 (1968).
(20) N. M. Bashara and D. W. Peterson, *J. Opt. Soc. Am.*, **56**, 1320 (1966).
(21) L. G. Schulz and F. R. Tanghelini, *J. Opt. Soc. Am.*, **44**, 362 (1954).
(22) J. D. E. McIntyre and D. E. Aspnes, *Surf. Sci.*, **24**, 417 (1971).
(23) E. B. Smith, C. S. Barnes, and P. W. Carr, *Anal. Chem.*, **44**, 1663 (1972).

RECEIVED for review June 18, 1979. Accepted January 25, 1980.

Application of Photothermal Spectroscopy to in-Situ Studies of Films on Metals and Electrodes

George H. Brilmyer and Allen J. Bard*

Department of Chemistry, The University of Texas at Austin, Austin, Texas 78712

The technique of photothermal spectroscopy (PTS) with improved instrumentation was used to study films, such as paints and dyes, on metal substrates. PTS was also used to monitor in situ the formation and spectra of surface layers on electrodes. PTS investigations of the electrodeposition of Cu and heptylviologen bromide on a Pt electrode are reported. The technique as described can detect surface layers ~75-100 monolayers. A one-dimensional thermal diffusion model of the PTS effect is also described.

The search for spectroscopic methods which can be used for opaque samples has led to investigations of techniques such as photoacoustic spectroscopy (PAS) (*1-5*) where absorption of radiation is detected by the pressure fluctuations induced in a gas by thermal changes in the sample. There is particular interest in possible spectroscopic techniques for the study of solid samples immersed in a liquid, such as electrodes in electrochemical cells. Such methods would complement the powerful electron spectroscopic techniques (*6, 7*), which require removal of the sample from the cell and placement in a high vacuum environment, and the widely-used spectroelectrochemical and reflectance techniques (*8, 9*), which place rather severe requirements upon the nature of the electrodes employed. While direct PAS techniques, utilizing microphone detectors are not very sensitive for measurements of solids immersed in liquids, recently described techniques employing piezoelectric detectors (*10*) appear quite promising. A recent report from this laboratory (*11*) introduced the technique of photothermal spectroscopy (PTS) in which a thermistor in contact with a sample is employed to detect temperature changes caused by radiationless transitions resulting from the absorption of light by the sample. By studying the relative temperature change as a function of irradiation wavelength (provided by a high intensity source), the absorption spectra of optically opaque samples can be obtained. The previously reported PTS studies have focused mainly on the characterization of various semiconducting materials (single crystal and polycrystalline) and the study of photoelectrochemical reactions at semiconductor electrodes (*12*).

The principles for the application of PTS to the in-situ study of metal electrodes is as follows. A highly polished metal electrode absorbs only a small amount of radiation (with the generation of heat) for most of the visible-near UV region. Therefore, when light-absorbing species are generated on or near the electrode, a photothermal signal will be obtained upon irradiation whose magnitude depends upon the molar absorptivity of the species, the amount of species generated, and the thermal properties of the system.

In this paper we present a theoretical model of the PTS effect and describe the application of PTS to studies of films (dyes and paints) on metal foil substrates as well as electrogenerated layers on platinum foil electrodes. The latter experiments involved the electrodeposition of copper and the formation of a precipitate of diheptylviologen radical cation bromide. Electrochemical experiments in which the spectra of generated layers and the variation of the PTS signal with potential during slow scan cyclic voltammetry were obtained, were employed to estimate detection limits for this technique.

EXPERIMENTAL

Apparatus. The basic cell used for the spectroelectrochemical experiments is shown in Figure 1. While the design is similar to that previously described (*11*), a differential thermistor arrangement was used to compensate for changes in ambient temperature. This change greatly improved base-line stability. One thermistor (the working thermistor) was attached to the rear of

0003-2700/80/0352-0685$01.00/0 © 1980 American Chemical Society

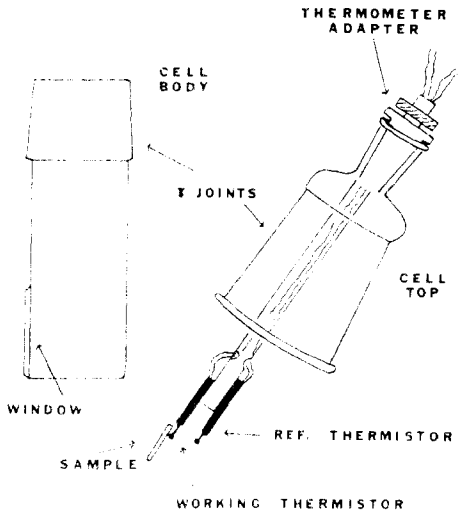

Figure 1. Cell used for photothermal spectroscopy and electrochemical studies (counter and reference electrodes are not shown)

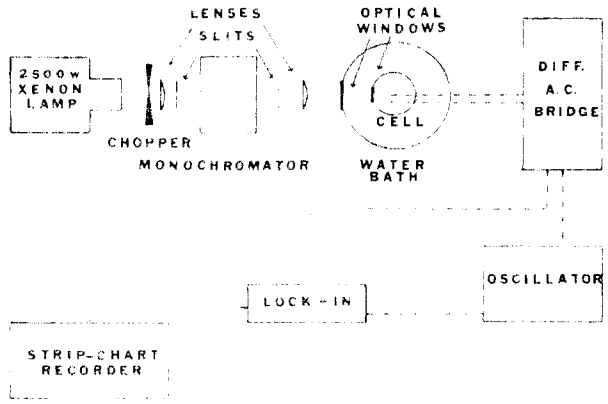

Figure 2. Block diagram of PTS instrumentation

the sample by an epoxy cement (Devcon Corp., Danvers, Mass.). The other thermistor (the reference thermistor) was held in place in the same manner near the working thermistor, but was not in contact with the sample. Neither thermistor was irradiated directly by the excitation beam during the experiment.

The instrumental arrangement used in these experiments is shown in Figure 2. The light source was a 2.5-kW short arc lamp housed in an Oriel Model LH-152N housing. A chopper consisting of a 10-inch aluminum disk was rotated at 1 rpm producing one 15-s light pulse every minute. The chopped beam was then focused onto the entrance slit of a Jarrell-Ash Monochromator (Model 82-410) and the resulting beam (10-nm band pass) was focused six inches from the exit slit using an $f/2$ quartz lens. The water bath and cell were positioned for maximum irradiation of the sample. The power spectrum of the resulting radiation, determined as before (*11*), had an average intensity of ~7 mW/cm^2 from 400 to 750 nm.

The thermistors (Victory Engineering Model 32A223), with nominal resistances of 2 kΩ and sensitivities of 78 Ω/K, were incorporated into a differential ac bridge constructed in this laboratory (Figure 3). The circuit is a slightly modified version of that used by Bonilla and Vassos (*13*). The bridge was driven by a 200-mV, 10-kHz signal from an oscillator (Hewlett-Packard, Model 650A) which showed a very stable output over long periods of time. The circuitry around and including OP-1 served as a differential amplifier with resistive and capacitive balancing for nulling purposes. The OP-2 circuit (10-kHz band pass filter) eliminated transients which otherwise degraded the S/N ratio at high sensitivities. OP-1 and OP-2 were TI-741 frequency compensated operational amplifiers. The relatively low noise and low drift of these amplifiers proved sufficient for these measurements. The ac bridge was used in conjunction with a Princeton Applied Research (PAR) Model 5204 lock-in amplifier whose resulting output signal (1.0 V full scale) was displayed on a Moseley Model 7100B strip chart recorder. The system as described has an overall sensitivity of 1.7 mV/°C. All electrochemical experiments were conducted with a PAR Model 173 potentiostat equipped with a PAR Model 179 digital coulometer and PAR Model 175 programmer. Cyclic voltammograms were displayed on a Houston Instruments model 2000 X-Y recorder.

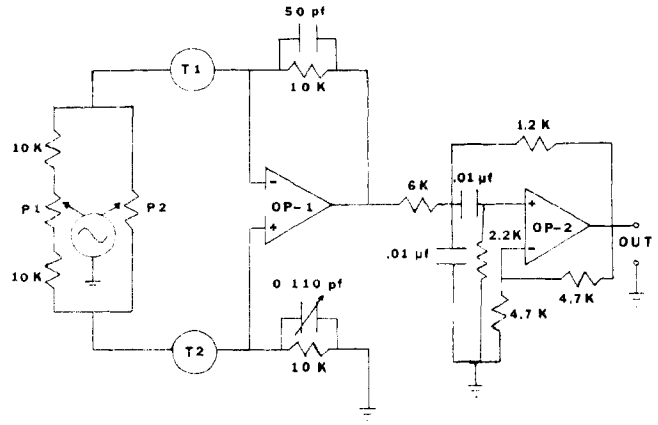

Figure 3. Differential ac bridge. Oscillator is 10 KHz (200 mV), OP-1 and OP-2 are TI-741 frequency compensated operational amplifiers. P1 and P2 are 500-Ω ten-turn potentiometers and T1 and T2 are a matched pair of thermistors (2 KΩ). Adapted from circuit in (*13*)

Chemicals. The enamel paints were manufactured by Testor Corp., Rockford, Ill. Zinc phthalocyanine, obtained from A. B. P. Lever, was used without further purification. $CuSO_4 \cdot 7H_2O$ (American Drug Chemical Co.), KBr (Fisher Scientific Co.) and 1,1′-dihepthyl-4,4′-bipyridinium dibromide (DHV^{2+}) (Aldrich Chemical Co.) were all used as received. All solutions for electrochemical studies were prepared with distilled water and degassed prior to use with prepurified nitrogen. The platinum foil used as substrate and electrode material (thickness, 0.001 in.) was polished with alumina (0.3 µm), rinsed with 95% ethanol, and then thoroughly rinsed with distilled water before use. The auxiliary electrode was a platinum wire coil and the reference electrode a saturated calomel electrode (SCE).

Procedure. Spectral characteristics of the enamel paints were obtained by applying an optically dense coating of each paint to the platinum substrate with the attached working thermistor. The photochemical response of the samples was obtained at a series of wavelengths (at 10-nm intervals); the spectra shown represent the temperature rise during the illumination period normalized to that of carbon black. Similar experiments were performed with vacuum deposited zinc phthalocyanine films of various thicknesses. The electrochemical experiments were carried out using a three-electrode cell. The placement of the Pt working electrode with attached thermistors permitted illumination of the electrode surface through the optical flats of the cell and water bath. The sensitivity was first adjusted by irradiating the clean Pt electrode with chopped monochromatic light, of wavelength corresponding to maximum absorbance of the electroplated material, and adjusting the lock-in amplifier and recorder sensitivites to produce a 1-inch deflection on the strip chart recorder. The species of interest was electrodeposited during the dark cycle at controlled potential and was detected from the PTS response during the light cycle. The absorption spectra of the films were obtained by varying the wavelength of the incident radiation after electrodeposition of a film of a known thickness. Alternately, the wavelength was held constant and the PTS signal studied as a function of film thickness.

RESULTS AND DISCUSSION

Theoretical Treatment of Photothermal Effect. We previously presented a simplified theoretical treatment of the PTS (*11*) and Lin et al. (*14*) recently described a thermal diffusion model of PTS. We present here a more detailed model of PTS, which differs in some respects from the previous model (*14*). Some preliminary tests of this model are also described. Our simplified model treats the effect as a one-dimensional diffusion-controlled heat transfer problem.

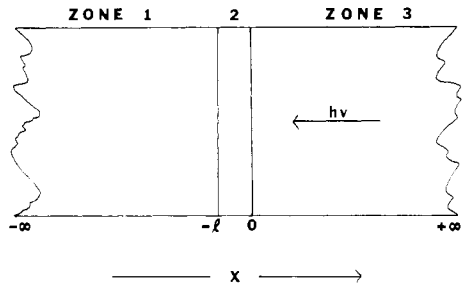

Figure 4. One-dimensional model for photothermal effect

It is assumed that the sample absorptivity, β, is very high (which is the case for the opaque samples considered here) so that all of the light is absorbed and converted to heat at the irradiated surface of the sample. Furthermore effects of surface roughness, convective heat transfer in the fluid surrounding the sample, and possible perturbation of the thermal gradients by the presence of the thermistor attached to the sample are neglected. The model is represented in Figure 4. The sample (zone 2) has a thickness, l, and extends from an x (the distance variable) of 0 (the irradiated surface) to $-l$ (the dark, thermistor, side). The surrounding medium, zones 1 and 2, extend from $0 \leq x < \infty$ and $-l \geq x > -\infty$. It is assumed that there is no surface resistance to heat flow between sample and surroundings; these are characterized by the thermal parameters K_i, the thermal conductivity (cal/cm·s·°C) and α_i, the thermal diffusivity (cm^2/s), where $\alpha_i = K_i/\rho_i C_{pi}$; ρ_i and C_{pi} are the density and heat capacity of material i respectively ($i = 2$ for sample, $i = 1,3$ for surroundings).

Irradiation of the sample with light of intensity I_0 (cal/s-cm^2) produces a corresponding heat flux Q

$$Q = I_0 (1 - e^{-\beta x}) \tag{1}$$

In this paper we assume $\beta \to \infty$, so that $Q = I_0$. Lin et al. (*14*) discuss the case of more transparent samples. The temperature in each zone, T_i, is a function of distance, x, and time, t, and is governed by the usual heat conduction equations (*15*):

$$\frac{\partial T_i(x,t)}{\partial t} = \alpha_i \frac{\partial^2 T_i(x,t)}{\partial x^2} \tag{2}$$

Initially the temperature is uniform in all zones; this was taken as zero to simplify the form of the final solutions (the choice of initial temperature does not affect the final results in terms of relative temperature changes). Thus

$$T_i = 0 \qquad t = 0 \text{ at all } x \tag{3}$$

The additional conditions for solution of the problem are equality of temperatures at the interfaces

$$T_3\,(0,t) = T_2\,(0,t) \tag{4}$$

$$T_1\,(-l,t) = T_2\,(-l,t) \tag{5}$$

and the balance conditions for the heat fluxes at the interfaces:

$$K_3 \left(\frac{\partial T_3}{\partial x}\right)_{x=0} - K_2 \left(\frac{\partial T_2}{\partial x}\right)_{x=0} = Q \tag{6}$$

$$K_1 \left(\frac{\partial T_1}{\partial x}\right)_{x=-l} - K_2 \left(\frac{\partial T_2}{\partial x}\right)_{x=-l} = 0 \tag{7}$$

These conditions are different than those of Lin et al. (*14*) who considered the case where the temperature of the surrounding medium remained constant during the experiment (i.e., $T_1(x,t) = T_3(x,t) = T_0$). The light pulse extends for a time $0 < t < \tau$. The general solution was obtained by the Laplace transform technique and is described in detail elsewhere (*16*). The solutions for the temperatures in the three zones during the light pulse are:

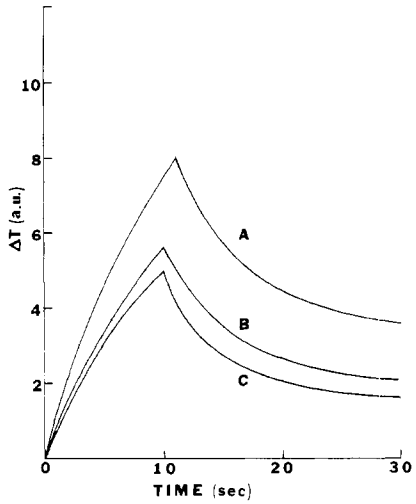

Figure 5. Calculated photothermal response for carbon (0.05 cm) in (A) air, (B) benzene, and (C) water

$$T_1(x,t) = \sum_{n=0}^{\infty} \frac{\left(\frac{2QK_2}{\alpha_2^{1/2}}\right)\left(\frac{K_1^2}{\alpha_1} - \frac{2K_1K_2}{(\alpha_1\alpha_2)^{1/2}} + \frac{K_2^2}{\alpha_2}\right)^n}{\left(\frac{K_1^2}{\alpha_1} + \frac{2K_1K_2}{(\alpha_1\alpha_2)^{1/2}} + \frac{K_2^2}{\alpha_2}\right)^{n+1}} \times$$

$$\left[2\left(\frac{t}{\pi}\right)^{1/2} e^{-(1/4t)[(l+2nl)/\alpha_2^{1/2} - (l+x)/\alpha_1^{1/2}]^2} - \left(\frac{l+2nl}{\alpha_2^{1/2}} - \frac{l+x}{\alpha_1^{1/2}}\right) \text{erfc}\left[\left(\frac{t^{-1/2}}{2}\right)\left(\frac{l+2nl}{\alpha_2^{1/2}} - \frac{l+x}{\alpha_1^{1/2}}\right)\right]\right] \tag{8}$$

$$T_2(x,t) = \sum_{n=0}^{\infty} \frac{Q\left(\frac{K_2}{\alpha_2^{1/2}} - \frac{K_1}{\alpha_1^{1/2}}\right)\left(\frac{K_1^2}{\alpha_1} - \frac{2K_1K_2}{(\alpha_1\alpha_2)^{1/2}} + \frac{K_2^2}{\alpha_2}\right)^n}{\left(\frac{K_1^2}{\alpha_1} + \frac{2K_1K_2}{(\alpha_1\alpha_2)^{1/2}} + \frac{K_2^2}{\alpha_2}\right)^{n+1}} \times$$

$$\left[2\left(\frac{t}{\pi}\right)^{1/2} e^{-(1/4t)[(2l+2nl+x)/\alpha_2^{1/2}]^2} - \left(\frac{2l+2nl+x}{\alpha_2^{1/2}}\right) \text{erfc}\left[\left(\frac{t^{-1/2}}{2}\right)\left(\frac{2l+2nl+x}{\alpha_2^{1/2}}\right)\right]\right] +$$

$$\frac{Q\left(\frac{K_2}{\alpha_2^{1/2}} + \frac{K_1}{\alpha_1^{1/2}}\right)\left(\frac{K_1^2}{\alpha_1} - \frac{2K_1K_2}{(\alpha_1\alpha_2)^{1/2}} + \frac{K_2^2}{\alpha_2}\right)^n}{\left(\frac{K_1^2}{\alpha_1} + \frac{2K_1K_2}{(\alpha_1\alpha_2)^{1/2}} + \frac{K_2^2}{\alpha_2}\right)^{n+1}} \times$$

$$\left[2\left(\frac{t}{\pi}\right)^{1/2} e^{(1/4t)[(2nl-x)/\alpha_2^{1/2}]^2} - \left(\frac{2nl-x}{\alpha_2^{1/2}}\right) \text{erfc}\left[\left(\frac{t^{-1/2}}{2}\right)\left(\frac{2nl-x}{\alpha_2^{1/2}}\right)\right]\right] \tag{9}$$

$$T_3(x,t) = \sum_{n=0}^{\infty} \frac{Q\left(\frac{K_2}{\alpha_2^{1/2}} - \frac{K_1}{\alpha_1^{1/2}}\right)\left(\frac{K_1^2}{\alpha_1} - \frac{2K_1K_2}{(\alpha_1\alpha_2)^{1/2}} + \frac{K_2^2}{\alpha_2}\right)^n}{\left(\frac{K_1^2}{\alpha_1} + \frac{2K_1K_2}{(\alpha_1\alpha_2)^{1/2}} + \frac{K_2^2}{\alpha_2}\right)^{n+1}} \times$$

$$\left[2\left(\frac{t}{\pi}\right)^{1/2} e^{-(1/4t)[(2l+2nl)/\alpha_2^{1/2} + x/\alpha_1^{1/2}]^2} - \left(\frac{2l+2nl}{\alpha_2^{1/2}} + \frac{x}{\alpha_1^{1/2}}\right)\operatorname{erfc}\left[\left(\frac{t^{-1/2}}{2}\right)\left(\frac{2l+2nl}{\alpha_2^{1/2}} + \frac{x}{\alpha_1^{1/2}}\right)\right]\right] +$$

$$\frac{Q\left(\frac{K_2}{\alpha_2^{1/2}} + \frac{K_1}{\alpha_1^{1/2}}\right)\left(\frac{K_1^2}{\alpha_1} - \frac{2K_1K_2}{(\alpha_1\alpha_2)^{1/2}} + \frac{K_2^2}{\alpha_2}\right)^n}{\left(\frac{K_1^2}{\alpha_1} + \frac{2K_1K_2}{(\alpha_1\alpha_2)^{1/2}} + \frac{K_2^2}{\alpha_2}\right)^{n+1}} \times$$

$$\left[2\left(\frac{t}{\pi}\right)^{1/2} e^{-(1/4t)(2nl/\alpha_2^{1/2} + x/\alpha_1^{1/2})^2} - \left(\frac{2nl}{\alpha_2^{1/2}} + \frac{x}{\alpha_1^{1/2}}\right)\operatorname{erfc}\left[\left(\frac{t^{-1/2}}{2}\right)\left(\frac{2nl}{\alpha_2^{1/2}} + \frac{x}{\alpha_1^{1/2}}\right)\right]\right] \quad (10)$$

The temperature profiles during the dark period following the light pulse ($t > \tau$) can be obtained by a similar approach using step function notation, i.e.,

$$Q = Q\,[1 - S_\tau(t)] \quad (11)$$

where $S_\tau(t)$ is the unit step function, $S_\tau(t) = 0$ $(t < \tau)$, $S_\tau(t) = 1$ $(t > \tau)$ (*17*). The general result for $T_1(x,t)$ is

$$T_1(x,t) = \frac{\left(\frac{2QK_2}{\alpha_2^{1/2}}\right)\left(\frac{K_1^2}{\alpha_1} - \frac{2K_1K_2}{(\alpha_1\alpha_2)^{1/2}} + \frac{K_2^2}{\alpha_2}\right)^n}{\left(\frac{K_1^2}{\alpha_1} + \frac{2K_1K_2}{(\alpha_1\alpha_2)^{1/2}} + \frac{K_2^2}{\alpha_2}\right)^{n+1}} \times$$

$$\left[2\left(\frac{t}{\pi}\right)^{1/2} e^{-(1/4t)[(l+2nl)/\alpha_2^{1/2} - (l+x)/\alpha_1^{1/2}]^2} - \left(\frac{l+2nl}{\alpha_2^{1/2}} - \frac{l+x}{\alpha_1^{1/2}}\right)\operatorname{erfc}\left[\left(\frac{t^{-1/2}}{2}\right)\left(\frac{l+2nl}{\alpha_2^{1/2}} - \frac{l+x}{\alpha_1^{1/2}}\right)\right]\right] -$$

$$\frac{\left(\frac{2QK_2}{\alpha_2^{1/2}}\right)\left(\frac{K_1^2}{\alpha_1} - \frac{2K_1K_2}{(\alpha_1\alpha_2)^{1/2}} + \frac{K_2^2}{\alpha_2}\right)^n}{\left(\frac{K_1^2}{\alpha_1} + \frac{2K_1K_2}{(\alpha_1\alpha_2)^{1/2}} + \frac{K_2^2}{\alpha_2}\right)^{n+1}} \times$$

$$\left[2\left(\frac{t-\tau}{\pi}\right)^{1/2} e^{-[1/4(t-\tau)][(l+2nl)/\alpha_2^{1/2} - (l+x)/\alpha_1^{1/2}]^2} - \left(\frac{l+2nl}{\alpha_2^{1/2}} - \frac{l+x}{\alpha_1^{1/2}}\right)\operatorname{erfc}\left[\left(\frac{(t-\tau)^{-1/2}}{2}\right)\left(\frac{l+2nl}{\alpha_2^{1/2}} - \frac{l+x}{\alpha_1^{1/2}}\right)\right]\right] \quad (12)$$

These equations allow calculation of the temperature profiles during the light pulse at any location, once the thermal constants for the sample and surroundings (*18*, *19*) and the sample thickness are specified. The thermistor response can

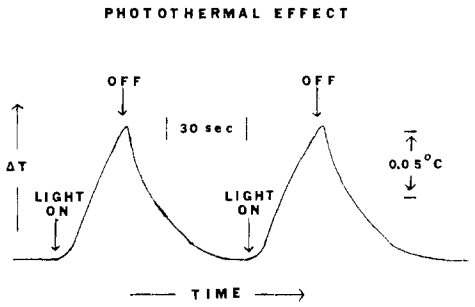

Figure 6. Photothermal response for red enamel on platinum foil (465 nm)

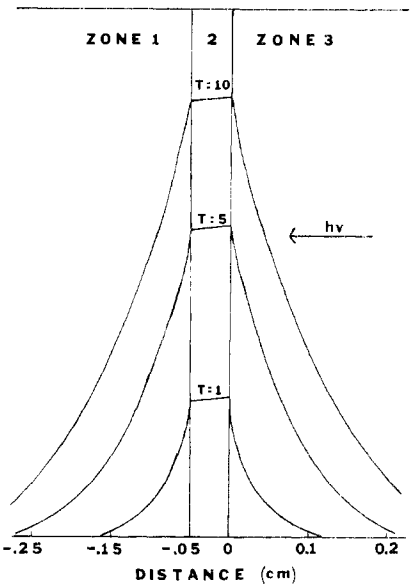

Figure 7. Calculated temperature profiles for carbon (0.05 cm) in water at various times. $Q = 1.0$; $l = 0.05$ cm

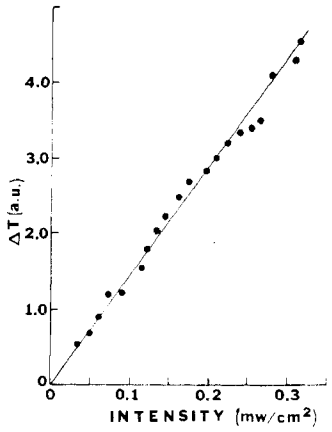

Figure 8. Experimental photothermal response for carbon (0.05 cm) in air as a function of polychromatic light intensity

Table I. Calculated and Observed Relative Temperature Changes for Carbon Sample in Various Media[a]

surrounding medium	ΔT calculated	ΔT measured
water	1.0	1.0
benzene	1.13	2.9
air	1.6	6.8

[a] Graphite, 0.05 cm thick.

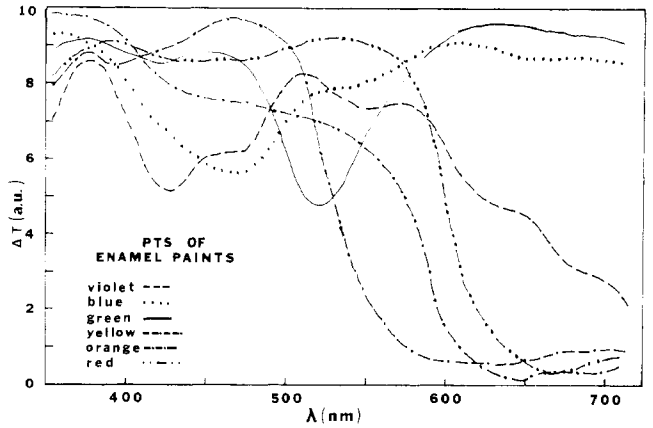

Figure 9. Corrected normalized photothermal spectra of enamel paints on platinum foil

be taken as proportional to the temperature change at $x = -l$. The calculated time response for light pulse on a carbon sample immersed in three different media (air, water, benzene), is shown in Figure 5. The shapes of these are quite similar to those found experimentally (e.g., Figure 6). Typical calculated temperature profiles during the light pulse for a carbon sample immersed in water are shown in Figure 7. Note that in this case, for a thin sample of high thermal conductivity, the temperature gradient within the sample is very small (i.e., the sample heats almost uniformly). Under these conditions the relative temperature change will be smaller, the higher the thermal conductivity of the sample, since more heat will be lost on the dark side of the sample. For example, the relative calculated temperature changes in air for samples of equal thickness of Cu, Ag, Pt, and graphite are 1.0, 1.2, 2.1, and 2.9, respectively.

The model predicts that the photothermal response will be directly proportional to the absorbed light intensity. The experimental results for the irradiation of a carbon sample in air illuminated with white light (Figure 8) support this prediction. The relative PTS signals should also be a function of the thermal conductivity, density, and heat capacity of the surrounding media. However the observed relative temperature changes were always much larger than those calculated, as shown in the results for the carbon sample in air, water, and benzene (Table I). These differences may be caused by convective effects which occur in the liquids and perhaps by differences in the rate of heat transfer at the interfaces. More elaborate models for PTS that incorporate such effects can be considered; however, solution of these will require numerical or digital simulation methods. The simple model given here, as well as that of Lin et al. (*14*) appear to provide at least satisfactory semiquantitative results.

PTS of Films. Enamel paint films were studied using PTS to evaluate the technique as applied to thick film characterization and identification. Paints were chosen because of their relatively large absorptivities, their ease of application to metal surfaces, and the possible analytical significance of this application. The paints were sprayed or brushed on the platinum foil substrate with attached thermistor. The sample was illuminated with very slowly chopped light as previously described and the individual photothermal signals displayed as a function of time (Figure 6). The magnitude of the PTS signals depends on the optical and thermal properties of the system. In this experiment the measured signals were relatively large and noise-free, because they were obtained in air with a substrate with high thermal conductivity. The photothermal spectra of the various paints were corrected for the spectral distribution of the xenon lamp. For convenience in presenting the data, the spectra were normalized with respect to the maximum response for each sample (Figure 9). The

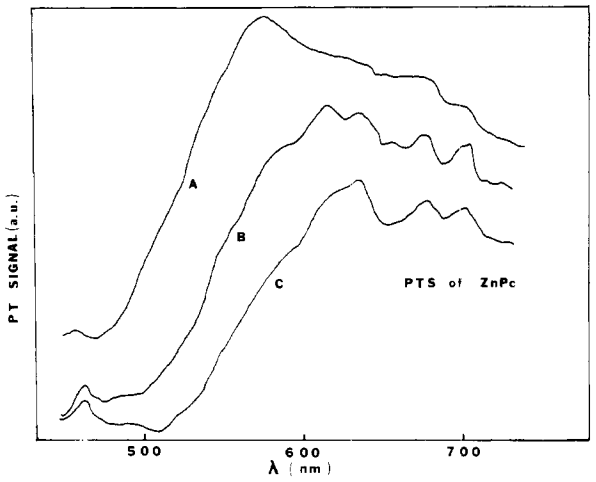

Figure 10. Corrected photothermal spectra of vacuum evaporated zinc phthalocyanine films; (A) ~3000 Å, (B) ~1000 Å, (C) ~200 Å

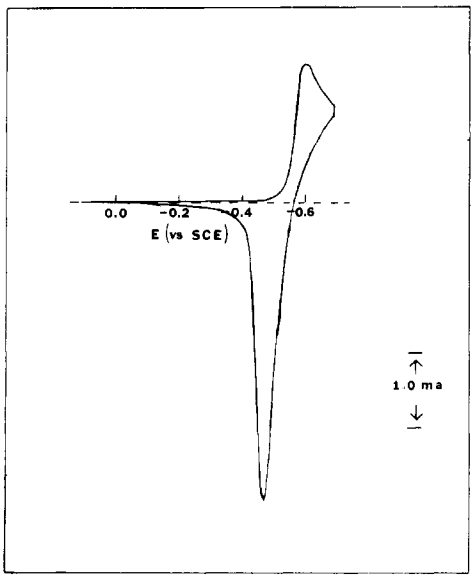

Figure 11. Cyclic voltammogram of aqueous solution containing 10^{-2} M DHV^{2+} and 0.2 M KBr at Pt electrode. Scan rate, 100 mV/s

actual magnitude of the PTS response depended on sample thickness, the nature of the surface, and sample absorptivity. The results shown are in qualitative agreement with those expected based on the color of each paint. Because it was difficult to control the thickness of the paint layers, no attempt was made to perform quantitative experiments of PTS signal vs. sample thickness. Even very thin paint smears produced signals well above the lower limit of detection of the technique. To investigate the effect of film thickness on PTS signal, thin films of zinc phthalocyanine (ZnPC) ($\epsilon_{max} \approx 10^5$ L cm^{-1} mol^{-1}) were investigated. In these experiments vacuum evaporation was used to deposit different amounts of ZnPc (corresponding to film thicknesses of 200–5000 Å). The PTS spectra (Figure 10) show a small apparent shift in the absorption maxima as a function of coverage toward the blue as the films became thicker. The observed PTS response depended on both the optical and thermal properties of film and substrate. Since in this technique the detector is at the rear of the sample, the maximum PTS signal is expected at a film thickness corresponding to optimum conditions for light absorption and heat transfer. At lower coverages, a decrease in the PTS signal results from decreased light absorption by the samples. At higher coverages, the signal will decrease because of the lower thermal conductivity of the sample. Since the light is absorbed at the front face of the sample, a greater fraction of the heat

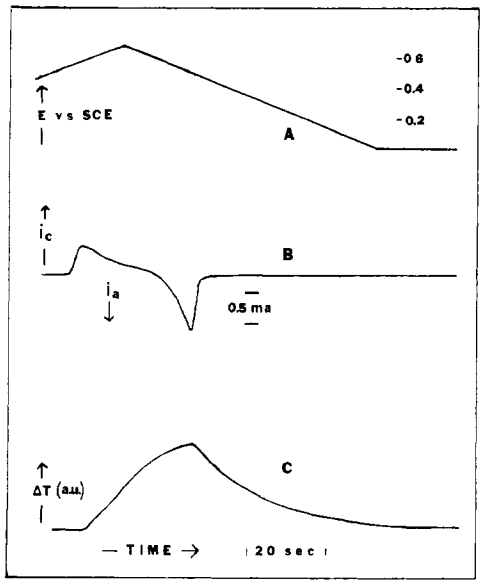

Figure 12. In-situ simultaneous photothermal response and current during cyclic voltammetry of DHV^{2+} at scan rate of 10 mV/s. (A) Potential program, (B) current, (C) photothermal response under constant illumination (500 nm)

produced is dissipated into the air rather than being conducted to the sample. A saturation effect can also occur because, as in PAS (*2, 20*), once a wavelength and thickness is attained where essentially all of the light is absorbed, the signal reaches its maximum value, and then becomes independent of λ. The minimum dye film thickness investigated was ~500 Å which yielded a PTS spectrum with a S/N ratio still above 10.

PTS of Electrodes. Electrogenerated films (metallic and organic) were produced on the front surface of the platinum substrate which was the working electrode of an electrochemical cell. The electrochemical experiments had the advantage of allowing the production of known amounts of materials and, hence, controlled film thicknesses, with good accuracy. This allowed quantitative studies as well as a more detailed investigation of the saturation effect previously observed. The electrochemical systems investigated were the electrodeposition of copper and the electroreduction (and subsequent precipitation of the bromide salt) of diheptylviologen. These two systems were chosen because the solutions are stable under irradiation and the two electrodeposited layers have very different chemical, optical, and thermal properties.

The reduction of bipyridinium ion DHV^{2+}

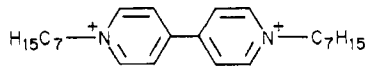

has been the subject of a number of studies in connection with electrochromic displays (*21, 22*), because upon reduction in bromide-containing solutions a dark red-violet precipitate of the radical cation bromide forms on the electrode (Equation 13).

$$DHV^{2+} + Br^- + e \rightarrow DHV^+ \cdot Br^- \qquad (13)$$

This precipitate can be removed from the electrode by oxidation. Thus in a typical cyclic voltammetric scan (Figure 11) the diffusion controlled reduction wave corresponds to precipitation of $DHV^+ \cdot Br^-$ and the surface oxidation wave to its disappearance. Simultaneous measurement of the current and the PTS signal under continuous irradiation during a single potential sweep cycle is illustrated in Figure 12. The PTS signal was monitored at 500 nm. Continuous irradiation of the clean Pt surface with the electrode held at −0.4 V vs. SCE first caused a rise in the temperature and then attainment of a steady-state value. During a cathodic sweep (10 mV/s), the PTS signal began to increase when cathodic current passed. After scan reversal and the start of the passage of anodic current, there was an appreciable time lag before the PTS signal began to decrease. This lag can be attributed to the saturation effect previously noted, the slow rate of heat transfer through the film, and the relatively slow response of the thermistor.

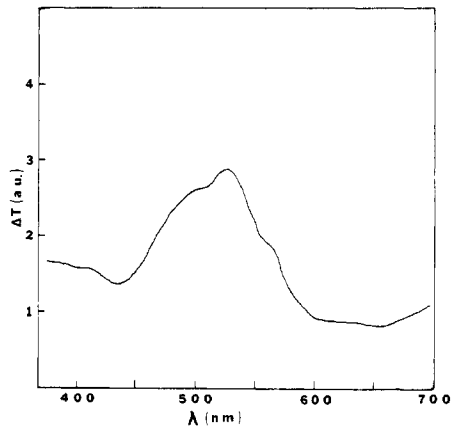

Figure 13. Corrected photothermal spectrum of $DHV^+ \cdot Br^-$ film on platinum electrode. The film thickness was maintained by pulsing (1 Hz) from −0.2 to −0.55 V vs. SCE

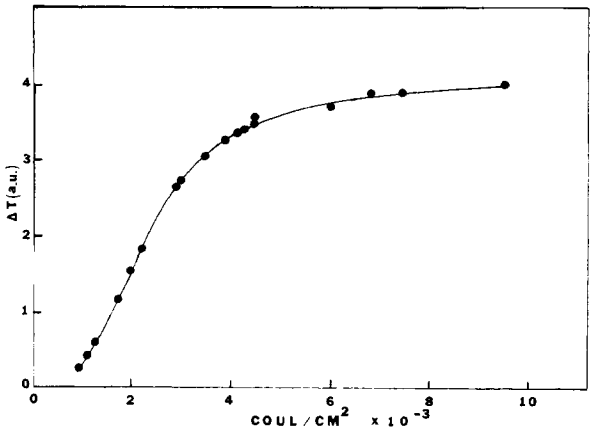

Figure 14. Photothermal response (at 500 nm) as function of integrated cathodic current (represented as $DHV^+ \cdot Br^-$ coverage) for controlled potential deposition on Pt at −0.50 V vs. SCE

The spectrum of the electrodeposited viologen film (Figure 13) was obtained by continuous pulsing of the electrode between −0.2 and −0.55 V vs. SCE at 1 Hz to produce and remove the film while the irradiation wavelength was swept. This procedure ensured that the viologen coverage remained low and constant during the experiment. When the coverage was greater than ~5 × 10^{16} molecules/cm^2 saturation effects, as found with ZnPc were noted; this resulted in an apparent shift in the absorption maxima. The effect of film thickness on the PTS signal was studied by a controlled potential deposition of the film and determination of the film thickness by measurement of the coulombs required with the assumption of uniform film formation. The results are shown in Figure 14. The lower limit of detection (for S/N of 1.0) corresponded to about 10^{-3} C/cm^2 (6.1 × 10^{15} molecules/cm^2) which represents several hundred monolayers of precipitate. The PTS signal was quite linear with coverage until attainment of thicknesses where saturation effects become important (~3.0 × 10^{16} molecules/cm^2). The nonzero intercept can be attributed either to a small amount of dissolution of the film or to the generation of the amount of $DHV^+ \cdot$ required to initiate precipitation.

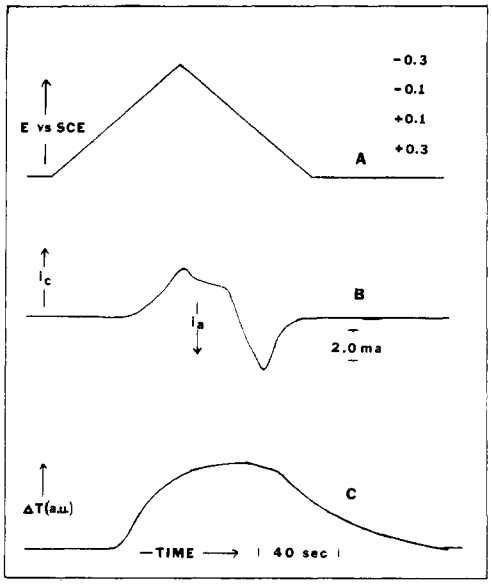

Figure 15. In-situ simultaneous photothermal response and current for cyclic voltammetry of Cu^{2+} at scan rate of 10 mV/s. (A) Potential program, (B) Current, (C) photothermal response under constant illumination (465 nm)

Similar experiments were also conducted for the electrodeposition of copper from a $CuSO_4$ solution. While this system showed the same type of response as DHV for the PTS signal and i with time (Figure 15), the spectral response could not be obtained. When photothermal spectra of the electroplated copper were recorded and corrected for the spectral distribution of the xenon lamp, a flat response was obtained, i.e., the electrodeposited Cu spectrum was the same as that of the lamp power spectrum. However, pure copper foil showed a PTS response which correlated well with that of bright copper obtained by reflectance measurements (*23*). The difference between bright and the electrodeposited copper can be attributed to the fact that electrodeposition produces a finely divided, dendritic, material which acts as a black body. The variation of PTS signal with amount of Cu deposited was investigated by deposition of different amounts of Cu at a potential of −0.3 V vs. SCE. The PTS response vs. coverage curve (Figure 16) is similar to that obtained with diheptylviologen except that at a Cu coverage corresponding to $\sim 2.0 \times 10^{17}$ molecules/cm^2, well into the saturation region, the PTS signal began to decrease. This decrease can be explained by noting that the formation of dendrites produces a material with a high surface area which results in a condition where energy is transferred more favorably into the solution in front of the electrode than through it to the detector. A theoretical model for the examination of such effects is currently under development.

CONCLUSIONS

The results show that PTS can be applied to the study of different types of films and that, over a limited range of coverage, the photothermal response is linear with film thickness. This suggests possible applications to analytical problems. For the two electroactive species examined, the lower limit for detection was of the order of 75–100 monolayers. While this sensitivity is adequate for a number of electrochemical applications, a sensitivity consistent with monolayer or submonolayer coverage is required for many problems. The sensitivity could be improved by instrumental changes such as more intense light sources (e.g., lasers), more sensitive thermal detectors, and light modulation or signal-averaging techniques (*24*). Another disadvantage of PTS in its present form for electrochemical applications is the slowness of the response caused by the rather long time constant

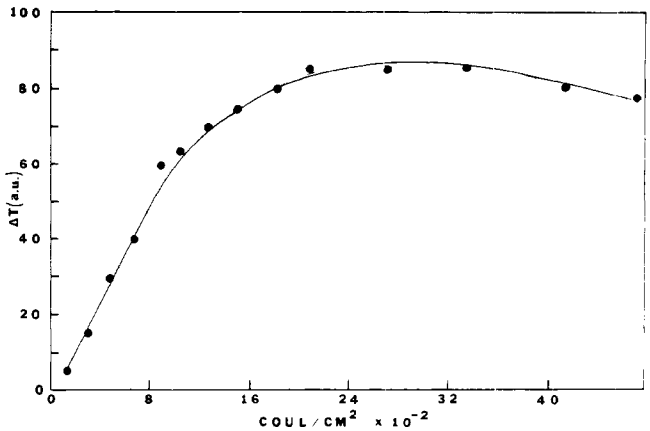

Figure 16. Photothermal response (at 465 nm) as function of integrated cathodic current (represented as Cu deposited) for controlled potential deposition on Pt at −0.30 V vs. SCE

of the thermistor employed. The response, currently of the order of seconds, could be improved by at least an order of magnitude, by use of faster thermistors and even further by the use of other temperature sensors. However, PTS has the advantage of simplicity and versatility. PTS can be applied to optically dense as well as optically transparent films. In both cases, the surface of the electrode need not be highly polished as required in reflectance or ellipsometric techniques. Since the detector is not affected by scattered or reflected light, problems associated with changes in refractive index ($f(\lambda)$) are minor. Electrochemical applications to the determination of efficiencies of photoelectrochemical cells and solid state photovoltaic cells also are possible (*25*).

LITERATURE CITED

(1) A. G. Bell, *Phil. Mag.*, **11**, 510 (1881).
(2) A. Rosencwaig and A. Gersho, *J. Appl. Phys.*, **47**, 64 (1976).
(3) A. Rosencwaig, *Anal. Chem.*, **47**, 592A (1976).
(4) R. C. Gray, V. A. Fishman, and A. J. Bard, *Anal. Chem.*, **49**, 697 (1977).
(5) M. J. Adams, A. A. King, and G. F. Kirkbright, *Analyst (London)*, **101**, 73 (1976).
(6) K. S. Kim, C. D. Seel, and N. Winograd, Proceedings of the Symposium on Electrocatalysis, M. W. Breiter, Ed., Electrochemical Society, Inc., Princeton, N.J., 1974, pp 242–57.
(7) J. Brinen and J. McClure, *Anal. Lett.*, **5**, 737 (1972).
(8) N. Winograd and T. Kuwana, "Electroanalytical Chemistry", A. J. Bard, Ed., Marcel Dekker, New York, 1974, Vol. 7.
(9) T. Kuwana, *Ber. Bunsenges. Phys. Chem.*, **77**, 858 (1973).
(10) R. E. Malpas and A. J. Bard, *Anal. Chem.*, **52**, 109 (1980).
(11) G. H. Brilmyer, A. Fujishima, K. S. V. Santhanam, and A. J. Bard, *Anal. Chem.*, **49**, 2057 (1977).
(12) A. Fujishima, G. H. Brilmyer, and A. J. Bard, in "Semiconductor Liquid-Junction Solar Cells", A. Heller, Ed., Electrochemical Society, Inc., Princeton, N.J. (Proceedings Vol. 77-3), 1977, pp 172–176.
(13) B. H. Vassos and A. Bonilla, *Chem. Instrum.*, **8**, 31 (1977).
(14) R. Tom, T. A. Moore, D. Benin, and S. H. Lin, *Chem. Phys. Lett.*, **66**, 390 (1979).
(15) H. S. Carslaw and J. C. Jaeger, "Conduction of Heat in Solids", Oxford University Press, 1947.
(16) G. H. Brilmyer, Ph.D. Dissertation, The University of Texas at Austin, 1979.
(17) R. V. Churchill, "Operational Mathematics", McGraw-Hill, New York, 1958, pp 25–28.
(18) W. H. Giedt, "Principles of Engineering Heat Transfer", D. Van Nostrand, Princeton, N.J., 1957.
(19) A. G. Worthing and D. Halliday, "Heat", John Wiley and Sons, New York, 1948.
(20) R. B. Somoano, *Angew. Chem., Int. Ed. Engl.*, **17**, 238 (1978).
(21) H. T. van Dam and J. J. Ponjeé, *J. Electrochem. Soc.*, **121**, 1555 (1974).
(22) R. T. Jasinski, *J. Electrochem. Soc.*, **124**, 637 (1977).
(23) F. A. Jenkins and H. E. White, "Fundamentals of Optics", 3rd ed., McGraw-Hill, New York, 1957.
(24) A. Fujishima, H. Masuda, K. Honda, and A. J. Bard, *Anal. Chem.*, preceding paper in this issue.
(25) A. Fujishima, Y. Maeda, K. Honda, G. H. Brilmyer, and A. J. Bard, *J. Electrochem. Soc.*, **127**, 840 (1980).

RECEIVED for review June 18, 1979. Resubmitted November 13, 1979. Accepted January 25, 1980. The support of this research by the U.S. Army Research Office—Durham is gratefully acknowledged.